Macular Function in Eyes with Open-Angle Glaucoma Evaluated by Multifocal Electroretinogram

Vincenzo Parisi,[1] *Lucia Ziccardi,*[1] *Marco Centofanti,*[1,2] *Lucia Tanga,*[1] *Geltrude Gallinaro,*[3] *Benedetto Falsini,*[4] *and Massimo G. Bucci*[1]

Purpose. To evaluate macular function in patients with open-angle glaucoma (OAG) by means of multifocal electroretinogram (mfERG).

Methods. Twenty-four OAG patients (mean age 54.6 ± 9.1 years) and 14 age-similar controls were enrolled. OAG patients had intraocular pressure (IOP) less than 18 mm Hg with topical medical treatment, 24-2 visual field (Humphrey Field Analyzer [HFA]) with mean deviation (MD) between −2 and −12 dB, and corrected pattern standard deviation (CPSD) between +2 and +10 dB and no history or presence of cataract and/or macular disease. MfERGs in response to 61 M-stimuli presented to the central 20° of the visual field were assessed in OAG patients (24 eyes) and in controls (14 eyes). Ring (R) analysis was performed every five retinal eccentricities in areas between the fovea and midperiphery: 0° to 2.5° (R1), 2.5° to 5° (R2), 5° to 10° (R3), 10° to 15° (R4), and 15° to 20° (R5). MfERG response amplitude density of the N1-P1 components (N1-P1 RAD, nV/deg^2) and P1 implicit time (P1 IT, ms) of the first-order binary kernel were measured for each ring.

Results. OAG patients showed a significant ($P < 0.01$) decrease in N1-P1 RADs and an increase in P1 IT in both R1 and R2 with respect to controls. The reduction in N1-P1 RADs was significantly ($P < 0.01$) correlated with HFA MD and CPSD. No other significant differences between OAG and controls were found.

Conclusions. OAG patients show macular dysfunction detectable by the mfERG technique. Since the mfERG N1-P1 component is thought to be generated by preganglionic elements (photoreceptors and OFF bipolar cells), our data support the functional impairment of the neural generators of the macular region in patients with glaucoma. (*Invest Ophthalmol Vis Sci.* 2012;53:6973–6980) DOI:10.1167/iovs.12-10256

Macular function can be evaluated electrophysiologically in a steady-state condition by recording of focal ERG (FERG), or in a dynamic status by recording of visual evoked potentials (VEPs) after photostress.[1–9] Both techniques have been used to study macular function in patients affected by open-angle glaucoma (OAG).[10,11] In OAG patients, FERG and VEP abnormalities have been described.[10,12] In particular, Machida et al.[11] saw an abnormality in the ERG that was ascribed to ganglion cells.

Two concerns exist about OAG macular damage and the electrophysiological evaluation. First, in OAG patients, pattern ERG (PERG) recordings showed an impairment of the ganglion cells and their fibers,[13,14] while FERG recordings suggested a dysfunction of preganglionic elements secondary to the pressure damage.[12,15,16] Second, a focal stimulus, testing local regions, has been used to study the retinal damage in OAG.[17]

PERG and FERG responses, however, cannot provide a measure of pathological changes in different retinal areas or a topographical assessment of retinal activity. The multifocal ERG (mfERG), instead, can examine the retina giving a clear indication of central and peripheral electrical responses.[18] The multifocal technique allows detection of the bioelectric responses obtained from localized retinal areas and in particular from the macular region, which are driven largely by the preganglionic components, for the greatest cone cell density.[19]

Moreover, while FERG allows the electrophysiological evaluation of preganglionic elements in response to luminance stimuli presented in a restricted part of the central retina (4–9 retinal degrees),[1,2,20] the mfERG technique is useful for assessing responses of several different retinal areas enclosed between 1° and 20° of eccentricity from the fovea.[21–23] In fact, while the FERG recording collects the contribution from the entire macular region, mfERG ring analysis allows separating selective measures of bioelectrical responses obtained from localized macular areas.[22,23] This means that recording mfERG, testing visual acuity, and performing automated visual field analysis make it possible to explore the entire central retina and, through appropriate data analysis, to receive selective information regarding the function of localized retinal regions.[22–24]

A kernel analysis applied to mfERG responses can be used to assess nonlinear functions of the visual system.[25] Since the first-order kernel of mfERG originates primarily in the preganglionic elements (photoreceptors and bipolar cells),[26] and several studies have reported altered mfERG in OAG and in ocular hypertension,[27–32] the present authors believed it would be interesting to clarify whether a dysfunction of the preganglionic elements may occur in OAG.

The aim of the present study was to evaluate the function of the preganglionic elements of the macular region by means of mfERG recordings with respect to the more peripheral retinal areas in OAG patients.

Methods

Patients

Fourteen eyes of 14 normal control subjects (range: 40–70 years, mean age 51.7 ± 6.0 years) and 24 eyes of 24 patients (range: 42–72 years,

From the [1]Fondazione G.B. Bietti - Istituto di Ricovero e Cura a Carattere Scientifico (IRCCS), Rome, Italy; the [2]Clinica Oculistica, Università di Roma Tor Vergata, Rome, Italy; the [3]Casa di cura San Domenico, Rome, Italy; and the [4]Istituto di Oftalmologia, Università Cattolica del Sacro Cuore, Rome, Italy.

Submitted for publication May 24, 2012; revised July 23 and September 6, 2012; accepted September 6, 2012.

Disclosure: **V. Parisi**, None; **L. Ziccardi**, None; **M. Centofanti**, None; **L. Tanga**, None; **G. Gallinaro**, None; **B. Falsini**, None; **M.G. Bucci**, None

Corresponding author: Lucia Ziccardi, Fondazione G.B. Bietti - IRCCS, Via Livenza 3, 00198, Roma, Italy; luxzic@hotmail.com.

mean age 54.6 ± 9.1 years) affected by OAG were examined. Each patient had previous experience with automated perimetry (at least six reliable examinations within the previous 3 years). OAG eyes were selected from a large population of OAG patients ($n = 187$) on the basis of the inclusion criteria (see below).

Normal subjects had intraocular pressure (IOP) ≤21 mm Hg; best corrected visual acuity of 0.0 logarithm of the minimum angle of resolution (logMAR) with a refractive error between −2.00 and +2.00 spherical equivalent; normal 24-2 full threshold visual field (Humphrey Field Analyzer [HFA] 740; Zeiss, San Leandro, CA) with a mean deviation (MD) ±0.5 dB and corrected pattern standard deviation (CPSD) <1 dB; and no ocular, metabolic, or neurological diseases. The calculation of MD involves averaging the differences between the measured sensitivities and the age-adjusted normal sensitivities (total deviations) at each test point, thereby describing the general depression or elevation of the field. The CPSD describes the spread of these total deviations and represents the asymmetry of the visual field.[33] The foveal threshold (FT) describes the measurement of the foveal sensitivity with an initial stimulus intensity of 30 dB.[34]

Inclusion criteria for OAG patients were as follows:

- IOP >23 mm Hg and <28 mm Hg (average of the two highest readings of the daily curve, from 8:00 AM to 6:00 PM, six independent readings, one every 2 hours) without medical treatment
- HFA with MD between −2 and −12 dB; CPSD between +2 and +10 dB; false-positive rate and false-negative rate each less than 20%
- Ability to maintain a stable fixation comparable to that of normal subjects (fixation loss rate ranging between 4% and 6%)
- Corrected visual acuity ranging from 0.0 to 0.1 logMAR
- One or more papillary signs on conventional color stereo slides: the presence of a localized loss of neuroretinal rim (notch), thinning of the neuroretinal rim, generalized loss of optic rim tissue, optic disc excavation, vertical or horizontal cup/disc ratio greater than 0.5, cup–disc asymmetry between the two eyes greater than 0.2, peripapillary splinter hemorrhages
- Refractive error (when present) between −2.00 and +2.00 spherical equivalent
- No previous history or presence of any ocular disease involving cornea and lens: in particular no evidence of early cataract (patients were classified as NO1, NC1, C1, and P1 according to the Lens Opacities Classification System III charts)[35]
- No previous history or presence of early signs of maculopathy and positive recording of Amsler test. The macular clinical evaluation was based on slit-lamp and indirect ophthalmoscopic examination using +90–+78 D no-contact lens (Volk Optical, Mentor, OH) after pupillary dilatation using tropicamide 1%.[23,24] Also, a 30° color fundus photograph centered on the fovea was taken. In addition, the absence of morphological changes in the macular region was assessed by macular optical coherence tomography (OCT) scan (Spectralis OCT; Heidelberg Engineering, Dossenheim, Germany)
- No previous history or presence of detectable spontaneous eye movements (i.e., nystagmus)
- No previous history or presence of diabetes, optic neuritis, any disease involving the visual pathways, or drug intake that can interfere with macular function
- Pupil diameter ≥3 mm without mydriatic or miotic drugs

Since it is known that the electrophysiological responses can be modified by the pharmacological reduction of IOP,[36–41] we enrolled only OAG patients with IOP values that were less than 18 mm Hg on beta-blocker monotherapy, maintained during the 8 months preceding the electrophysiological evaluation. IOP was assessed as the average of the two highest readings of the daily curve (from 8:00 AM to 6:00 PM, six independent readings, one every 2 hours).

The research followed the tenets of the Declaration of Helsinki. The protocol was approved by the local institutional review and ethical boards. Upon recruitment, informed consent was obtained from each subject enrolled in the study.

MfERG Recordings

VERIS Clinic 4.9 (Electro-Diagnostic Imaging, San Mateo, CA) was used for the mfERG assessment by our previously published method.[22–24]

The multifocal stimulus, consisting of 61 scaled hexagons, was displayed on a high-resolution, black-and-white monitor (size, 30 cm width and 30 cm height) with a frame rate of 75 Hz. The array of hexagons subtended 20° of the visual field. Each hexagon was independently alternated between black (1 cd/m^2) and white (200 cd/m^2) according to a binary m-sequence. This resulted in a contrast of 99%. The luminance of the monitor screen and the central fixation cross (used as target) was 100 cd/m^2. The m-sequence had 2^{13}-1 elements, and total recording time was approximately 4 minutes. Total recording time was divided into eight segments. Between segments, the subject was allowed to rest for a few seconds. Focusing lenses were used when necessary. In order to maintain a stable fixation, a small red target (0.5°), which was perceived by all subjects tested, was placed in the center of the stimulation field. At every mfERG examination, each patient positively reported that he or she could clearly perceive the cross fixation target. A camera provided an image of the eye, which was displayed on the computer screen so that fixation could be continuously monitored.

In all OAG tested subjects (OAG patients and controls), mfERGs were binocularly recorded in eyes with pupils maximally dilated to 7 to 8 mm after application of 1% tropicamide drops. Pupil diameter was measured by an observer (GG) by means of a ruler and a magnifying lens and stored for each tested eye. The cornea was anesthetized with 1% dicaine. MfERGs were recorded bipolarly between an active electrode (contact electrode Dawson-Trick-Litzkow [DTL]) and a reference electrode (Ag/AgCl electrode placed on the ipsilateral temple). A small Ag/AgCl skin ground electrode was placed at the center of the forehead. Interelectrode resistance was less than 3 KOhms. A binocular mfERG recording was preferred to help subjects have a stable target fixation. Eyes that exhaustively met the inclusion criteria were selected from each patient. When both eyes could be selected, the eye with the highest R1 to R5 N1-P1 response amplitude densities (RADs) was considered for statistical analysis (see below) according to the criteria used in our previously published work.[23]

The signal was amplified (gain 100,000) and filtered (band pass 1–100 Hz) by BM 6000 (Biomedica Mangoni, Pisa, Italy). After automatic rejection of artifacts (by VERIS Clinic 4.9 software), the first-order kernel response, K1, was examined. We analyzed the averaged response obtained from five concentric annular retinal regions (rings) centered on the fovea: from 0° to 2.5° (ring 1, R1), from 2.5° to 5° (ring 2, R2), from 5° to 10° (ring 3, R3), from 10° to 15° (ring 4, R4), and from 15° to 20° (ring 5, R5). For each obtained averaged response we evaluated the amplitude densities between the first negative peak, N1, and the first positive peak, P1 (N1-P1 RAD, expressed in nV/deg^2), and the implicit time of the first positive peak (P1 IT).

The MfERG ring analysis was selected to differentiate changes in the bioelectrical responses of the central macular region with respect to the more peripheral retinal areas.

Signal-to-Noise Ratio

MfERG signal-to-noise ratio (SNR) was estimated following the methodology discussed by Hood and Greenstein.[42] Briefly, a noise window equal in length to the period within which the response was analyzed was set as part of the record, but it was included in a temporal window that was assumed to contain little or no response. Signal temporal window for the mfERG was 0 to 80 ms[22]. SNR was defined as the ratio of the root mean square (RMS) signal plus noise (measured in the signal temporal window) of a given record to the mean RMS of all

Table 1. Clinical Characteristics Observed in OAG Patients

						R1		R2		R3		R4		R5	
OAG Patients	**A**	**VA**	**HFA MD**	**HFA CPSD**	**HFA FT**	**RAD**	**IT**	**RAD**	**IT**	**RAD**	**IT**	**RAD**	**IT**	**RAD**	**IT**
OAG 1	60	0	*−2.43*	*2.06*	34	114.8	*36.7*	48.8	*35.8*	27.9	35.8	21.6	36.4	18.2	38.2
OAG 2	58	0.1	*−9.26*	*8.98*	35	*35.7*	*34.2*	*33.5*	32.5	30	36.4	19.9	37.2	18.1	42.2
OAG 3	72	0	*−3.36*	*2.11*	34	87.1	32.4	53.8	32.5	39	32.5	23.8	36.3	18	40.6
OAG 4	48	0	*−2.98*	*2.09*	35	136.1	*36.7*	54.7	*35.7*	33.6	36.2	21.3	36.8	17.4	42.8
OAG 5	56	0.1	*−2.47*	*2.22*	36	*85.5*	*36.7*	*37.7*	*34.2*	27.8	34.2	19.7	34.2	17.3	41.6
OAG 6	61	0	*−5.41*	*5.21*	35	*53.3*	*34.2*	*27.3*	*34.5*	17.2	37.5	14.1	35.4	14	36.9
OAG 7	49	0	*−3.23*	*4.01*	34	120.1	*35*	*35.3*	*36.7*	25.5	35.8	16.4	35.8	13.9	42.4
OAG 8	43	0	*−4.72*	*3.48*	36	*60.4*	*36.7*	*36.6*	*35.8*	24.1	37.2	19.3	36.8	13.6	39.5
OAG 9	42	0	*−7.04*	*6.34*	33	*56.4*	*35.8*	*30.6*	*35.1*	17.3	33.3	14.7	33.3	13.5	33.5
OAG 10	62	0.1	*−3.26*	*2.51*	36	*76*	*38.3*	*29.2*	*35.2*	19.9	35.8	13.9	35.8	11.9	42.5
OAG 11	50	0.1	*−9.91*	*8.11*	35	*57.1*	*40.8*	*14.5*	*35*	19.6	30.8	13.1	30.8	11.3	42.1
OAG 12	68	0.1	*−10.29*	*9.44*	36	*29.2*	*35.8*	*19.1*	*36.1*	14.7	35.8	12.3	36.1	10.6	38.1
OAG 13	49	0.1	*−3.01*	*2.11*	33	*75.2*	*38.3*	*31.2*	*35*	17.6	35.8	12.5	36.6	10.5	40.8
OAG 14	59	0	*−3.4*	*2.28*	36	*63.7*	*38.3*	*30.8*	*35.2*	22.6	34.2	13.1	33.3	10.1	43.4
OAG 15	60	0	*−5.26*	*2.62*	34	109.8	33.1	*37.2*	32.5	15.3	34.4	14.7	34.3	17.6	38.8
OAG 16	52	0	*−3.13*	*2.22*	35	*78.1*	*39.2*	*35.3*	*35.8*	21.7	34.7	13.2	35.8	10.8	37.5
OAG 17	42	0	*−5.45*	*4.36*	34	*75.2*	*36.7*	*39*	*35.8*	24.1	31.7	18.3	34.7	14.5	40.3
OAG 18	60	0	*−4.19*	*2.41*	36	*74.7*	*34.2*	*39.3*	*34.2*	16.6	34.3	16.3	35.6	18.3	36.9
OAG 19	66	0	*−4.23*	*7.34*	35	*74*	*35*	*39*	32.5	21.1	34.3	14	35.3	11.4	37.5
OAG 20	42	0	*−2.86*	*3.46*	35	*61*	*35*	*32.4*	*36.7*	20.1	36.5	17.7	34.3	11.2	38.3
OAG 21	42	0	*−4.47*	*3.03*	*27*	*54.7*	28.3	*16.3*	29.2	15.2	32.5	15.8	32.5	14.3	32.5
OAG 22	62	0	*−7.76*	*4.41*	35	*54.2*	*38.3*	*30.8*	*36.7*	18.5	32.5	21.2	32.5	17.8	35.8
OAG 23	62	0	*−5.69*	*7.58*	*29*	*51.5*	31.7	*30.1*	31.7	23.1	31.7	14.7	29.2	14	36.7
OAG 24	60	0	*−5.26*	*2.62*	34	*35.3*	*38.3*	*29.5*	*38.3*	15.9	34.2	14	32.3	10.9	34.5
95% CL															
U			–	1.09	–	–	33.2	–	33.6	–	38.1	–	38.7	–	43.7
L			−0.79	–	32.2	86.7	–	39.7	–	14.1	–	7.1	–	9.6	–

Age (A, years); visual acuity (VA, logMAR); Humphrey 24-2 visual field (HFA); mean deviation (MD, dB); corrected pattern standard deviation (CPSD, dB); foveal threshold (FT, dB); mfERG N1-P1 response amplitude density (RAD, nV/deg^2); mfERG P1 implicit time (IT, milliseconds). R1 through R5 refer to five concentric annular retinal regions (rings) centered on the fovea: R1: 0° to 2.5°; R2: 2.5° to 5°; R3: 5° to 10°; R4: 10° to 15°; R5: 15° to 20°. 95% confidence limits (CL). Normal limits obtained from control subjects by calculation of mean values +2 SD (upper limit, U) for IT and CPSD, and mean values −2 SD (lower limit, L) for MD, FT, and RAD. Values in italics are the ones outside normal limits.

noise windows (61 for the mfERG). A SNR $\geq$3 was accepted for mfERG measurements. A recordable response had to have a SNR $\geq$3.

Statistics

For all parameters, a 95% confidence limit was obtained from age-similar normal subject data by calculation of mean values $\pm$2 standard deviations (SD): Mean values +2 SD were calculated for CPSD and ITs, and mean values −2 SD for MD, FT, and RADs.

Pearson's correlation was applied to compare FT, MD, and CPSD measurements of Humphrey perimetry with mfERG R1 to R5 N1-P1 RADs and P1 ITs. MfERG N1-P1 RAD and P1 IT values underwent logarithmic transformation to better approximate a normal distribution.

Differences of perimetric (HFA MD, CPSD, and FT) and electrofunctional parameters (mfERG R1–R5 N1-P1 RADs and P1 ITs) between control and OAG groups were evaluated by a one-way analysis of variance (ANOVA).

In all analyses, a P value lower than 0.01 was considered to be statistically significant.

Results

The clinical characteristics of OAG enrolled eyes, including demographic, perimetric, and electrophysiological data, are reported in Table 1.

Figure 1 shows examples of mfERG recordings (all traces and ring traces) and relative HFA performed on one control eye and on three different OAG eyes.

Table 2 reports the mean data and statistical analysis of age, as well as all perimetric and electrophysiological values observed in control and OAG eyes. The number of normal or abnormal values for HFA FT, MD, and CPSD, and mfERG N1-P1 RADs and P1 ITs detected in the OAG group is also reported.

Considering the individual outcomes, two OAG eyes presented HFA FT abnormal values. In ring 1, 19 and 20 eyes were abnormal for N1-P1 RADs and P1 ITs, respectively. In ring 2, abnormal values for N1-P1 RADs and P1 ITs were found in 21 and 18 eyes, respectively. In the more peripheral rings (R3, R4, and R5), all OAG eyes showed normal N1-P1 RADs and P1 ITs.

In Figures 2 and 3, individual values of N1-P1 RAD and P1 IT recorded in OAG eyes from ring 1 and ring 2 are plotted as a function of corresponding mean values of HFA MD and CPSD, respectively.

In ring 1 and ring 2, the reduced N1-P1 RADs were significantly ($P < 0.01$) correlated with the HFA MD and CPSD. No statistically significant correlations ($P > 0.01$) were found between P1 ITs and perimetric (HFA MD and CPSD) parameters or between HFA FT and N1-P1 RADs or P1 ITs.

In the more peripheral rings (R3, R4, and R5), no statistically significant correlations ($P > 0.01$) were found between perimetric (HFA FT, MD, and CPSD) and electrophysiological (N1-P1 RADs or P1 ITs) data.

On average, in OAG eyes, mfERG N1-P1 RADs and P1 IT values differed significantly ($P < 0.01$) from controls exclusively in ring 1 (0–2.5°) and ring 2 (2.5–5°). No significant ($P > 0.01$) differences between OAG and control eyes in FT, and in

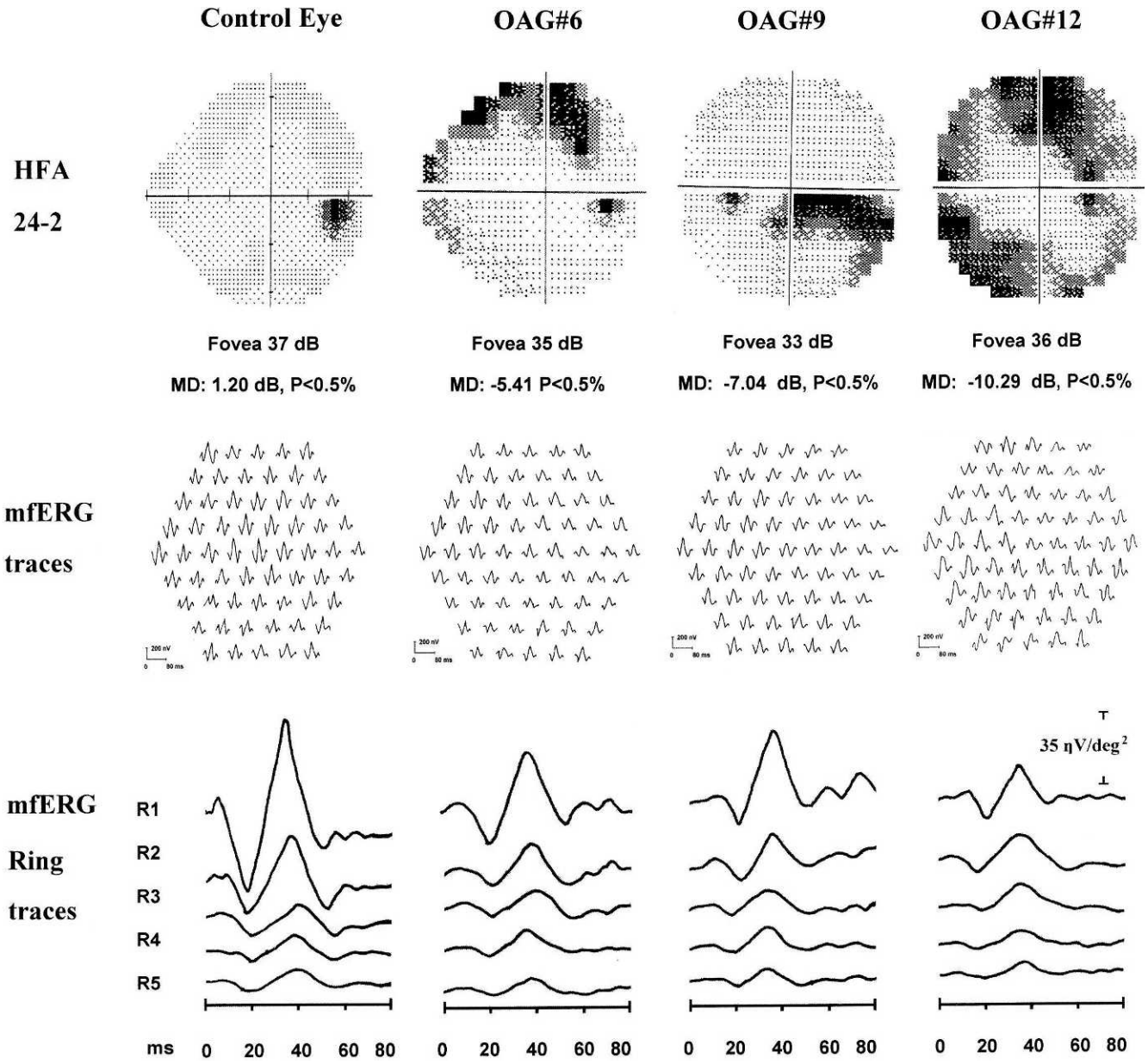

Figure 1. Examples of visual fields (Humphrey 24-2) and relative mfERG trace arrays for 61 hexagons and ring traces from one control and three OAG eyes. R1 to R5 refers to five concentric annular retinal regions (rings) centered on the fovea: R1: 0° to 2.5°; R2: 2.5° to 5°; R3: 5° to 10°; R4: 10° to 15°; R5: 15° to 20°.

the mfERG parameters (N1-P1 RADs and P1 ITs) in the more peripheral rings (R3, R4, and R5), were observed.

Discussion

Our aim was to assess the function of the preganglionic elements of the macular region in OAG patients by evaluating electrophysiological (mfERG) responses.

With respect to controls, in the OAG eyes with IOP values <18 mm Hg with topic beta-blocker monotherapy, a significant reduction of mfERG N1-P1 RADs was detected exclusively in R1 and R2 (0–5 central degrees), as well as a significant increase of P1 ITs. This may suggest a dysfunction selectively localized in the macular area. Because of our careful observation of control subjects and OAG patients during the mfERG recording (see our very stringent inclusion criteria), we believe that the observed abnormalities cannot be ascribed to losses of fixation or to the presence of early cataract or maculopathy. Our results are in agreement with previous suggestions obtained by psychophysical (color vision and contrast sensitivity) and other electrophysiological (VEPs after photostress, FERG, and PERG) measurements showing macular impairment in glaucoma patients.[10,11,15,17,43] Since the cited electrophysiological techniques (VEPs after photostress, FERG, and PERG) cannot provide a measure of functional changes in localized retinal areas within the macular region, we analyzed the mfERG responses that are able to provide information about the function of preganglionic elements from areas enclosed between 0° and 20° of eccentricity from the fovea.[18]

In fact, according to a framework proposed by Hood,[26] a disease that acts largely at the photoreceptoral level will decrease the amplitude of the mfERG, while damage of the

Table 2. Mean Values ± SD of Age (years), HFA 24-2 MD (dB), CPSD (dB), and FT (dB), and mfERG RAD (nV/deg^2) and mfERG P1 IT (ms) Values Observed in Control Eyes (C) and OAG Eyes

				ANOVA OAG versus C			
		C, $N = 14$	OAG, $N = 24$	$F_{1,37}$	P	Nr	Ab
	Age	51.7 ± 6.0	54.6 ± 9.13	1.12	0.296		
HFA	MD	−0.554 ± 0.928	−4.842 ± 2.38	41.1	<0.001	0	24
HFA	CPSD	1.30 ± 0.17	4.19 ± 2.44	19.36	<0.001	0	24
HFA	FT	35.6 ± 1.74	34.3 ± 2.18	3.67	0.0632	22	2
R1	RAD	118.3 ± 15.80	71.6 ± 27.06	34.63	<0.001	5	19
R1	IT	30.2 ± 1.55	35.8 ± 2.74	47.91	<0.001	4	20
R2	RAD	47.3 ± 3.80	33.8 ± 9.81	24.45	<0.001	3	21
R2	IT	30.7 ± 1.47	34.7 ± 2.01	42.09	<0.001	6	18
R3	RAD	22.8 ± 4.33	22.0 ± 6.19	0.18	0.673	24	0
R3	IT	33.2 ± 2.47	34.5 ± 1.85	3.40	0.073	24	0
R4	RAD	20.2 ± 6.54	15.3 ± 4.23	5.33	0.027	24	0
R4	IT	32.8 ± 2.96	34.6 ± 2.05	4.90	0.033	24	0
R5	RAD	16.3 ± 3.33	14.1 ± 9.98	4.42	0.043	24	0
R5	IT	37.9 ± 2.87	38.9 ± 3.06	0.99	0.327	24	0

The RADs and ITs were derived from five concentric annular retinal regions (rings) centered on the fovea. We analyzed the N1-P1 RADs derived from 0° to 2.5° (R1), from 2.5° to 5° (R2), from 5° to 10° (R3), from 10° to 15° (R4), and from 15° to 20° (R5). ANOVA = one-way analysis of variance between groups, $F_{1,37}$. *N*, number of eyes; Nr, number of eyes inside the normal limits; Ab, number of eyes outside the normal limits. Normal limits were obtained from control subjects by calculation of mean values +2 SD for IT and CPSD and mean values −2 SD for MD, FT, and RADs.

inner retina (i.e., amacrine cells, ganglion cells, and their connections) and the optic nerve head can only alter the mfERG waveform, producing small changes in amplitude.[27] Because damage of the ganglion cells or optic nerve does not decrease the mfERG amplitude, an abnormal mfERG provides strong evidence for preganglionic dysfunction.[19]

In particular, the outer and partially inner retinal layers have been debated as the most probable generators of the mfERG first-order kernel responses.[44] Hood et al. also described the first-order kernel as originating from photoreceptors and bipolar cells, in a study of the blockage of signal transmission to ON bipolars in nonhuman primates, as a working model of the human mfERG.[45] Accordingly, we studied the first-order kernel of mfERG responses selectively, also following previous studies reporting that deficits of the outer retinal components in glaucomatous eyes are specifically reflected in disorders of

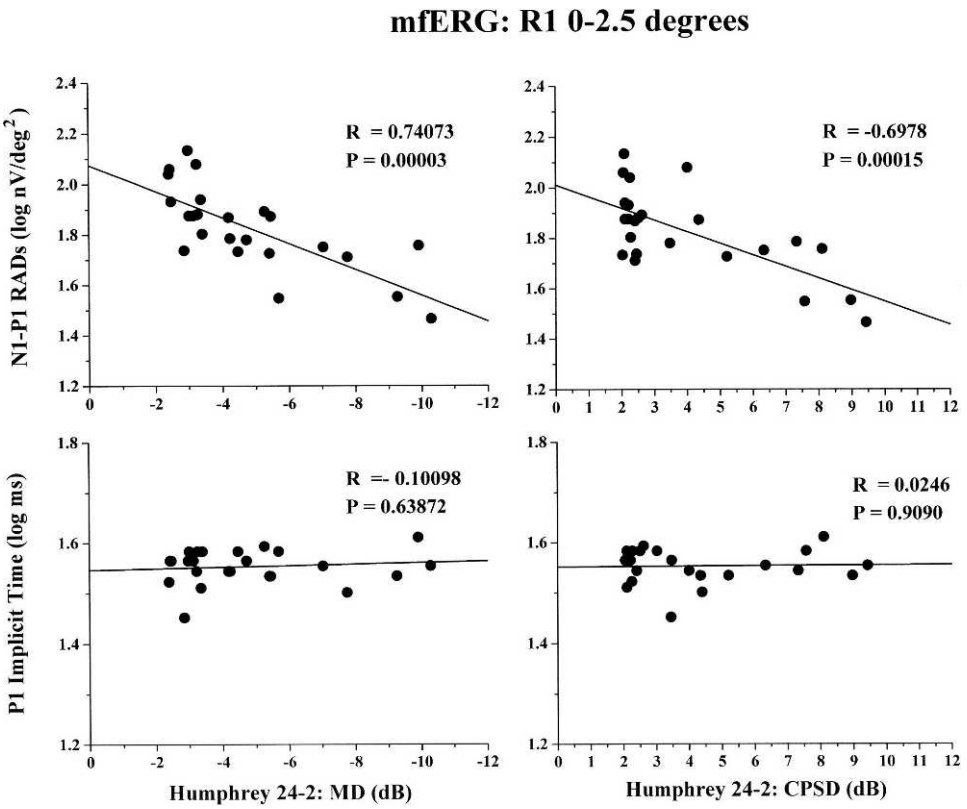

Figure 2. Individual mfERG N1-P1 response amplitude densities (RADs) and P1 implicit time recorded in the central 0° to 2.5° (ring 1) plotted against the corresponding values of MD and CPSD of the Humphrey 24-2 visual field in OAG eyes. Pearson's test was used for the linear regression.

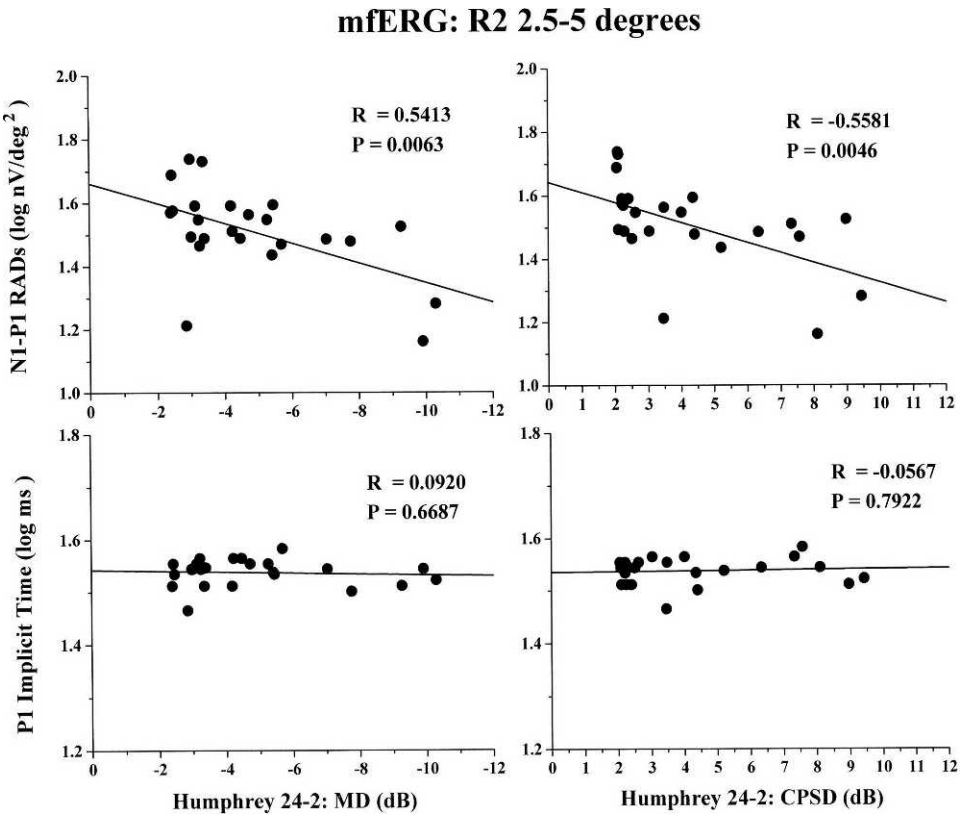

Figure 3. Individual mfERG N1-P1 response amplitude densities (RADs) and P1 implicit time recorded in the central 2.5° to 5° (ring 2) plotted against the corresponding values of MD and CPSD of the Humphrey 24-2 visual field in OAG eyes. Pearson's test was used for the linear regression.

the first-order kernel.[46,47] A general depression of the first-order kernel in OAG eyes has also been found by Vaegan and Buckland,[48] who suggested a uniform reduction in mfERG responses related to choriocapillary perfusion deficit and microcirculatory damage. This is in agreement with histological studies in postmortem human eyes, which describe a lower density of capillaries of the choriocapillaris in the macular choroid of OAG patients when compared to control eyes.[49]

Our remarkable finding consisted of an impairment localized in the 5 central degrees with a functional sparing of those preganglionic elements enclosed between 5 and 20 central degrees. This suggests a selective dysfunction of the foveal cell population. Nevertheless, this impairment is not sufficient to lead to a loss in sensitivity. In fact, only two of our OAG patients showed a reduction in the HFA FT, which was not statistically different between OAG and control subjects.

The observed dysfunction of the innermost area of the macular region is supported by recent findings suggesting morphological changes of the integrity of the cone outer segments in OAG patients with central visual defects. These structural abnormalities, which are potentially due to underlying decreased choroidal blood flow in the macula, were documented via reduced directional reflectance of foveal cone photoreceptors.[50] Additionally, histological studies by Nork et al.[51] have described signs of photoreceptoral swelling, not loss, in human outer retinas from OAG eyes, suggesting that changes of cone morphology are due to chronically elevated intraocular pressure. The authors proposed a mechanism of cone ischemia due to reduced choroidal blood flow in OAG eyes, leading to a reduced reuptake of glutamate. The high levels of extracellular glutamate would eventually result in secondary overstimulation and loss of second-order neurons and retinal ganglion cells. In this regard, Pelzel et al.[52] described a reduction in the expression of red/green and blue cone opsin in monkey retinas with chronic ocular hypertension by means of a quantitative mRNA analysis and in situ hybridization studies. However, they did not observe a rodopsin mRNA loss, thus concluding that ocular hypertension leading to glaucoma selectively affects cone photoreceptors of the outer retina. Nevertheless, these studies did not provide direct information about morphological changes exclusively localized in the foveal region. In the past, there was an extensive debate surrounding this argument. In fact, previous histological studies conducted on human glaucomatous eyes reported either photoreceptor preservation[53] or photoreceptor loss.[54] Also electrophysiological reports vary greatly. Studies conducted with full field/flash ERG in glaucoma have shown changes in scotopic and/or photopic responses,[55,56] thereby suggesting generalized photoreceptor damage; however a more recent study in experimental glaucoma reported normal photopic amplitude parameters.[57] In addition, the regional retinal functional impairment in glaucoma has been argued for years. Previous mfERG and multifocal pattern ERG studies reported limited success in localizing inner retinal layer damage in OAG,[58–61] and only recent evidence has shown regional outer retinal dysfunction in the central 24° in advanced glaucoma.[62] Therefore, at present, the mechanisms inducing the dysfunction of foveal photoreceptors in OAG still remain unclear.

We used two rather overlapping methods to explore the same area (the mfERG was derived from the central 20°, and the HFA explored the central 24°), but we did not aim to compare results provided by psychophysical (HFA 24-2) and electrophysiological (mfERG) techniques. In fact, in our study, we correlated the reduction of the N1-P1 mfERG amplitudes and the increase of P1 IT detected in the two more central

rings (R1–R2) with the generally used perimetric indices of glaucomatous damage (HFA MD and CPSD),[63] exclusively to assess whether the dysfunction observed in the macular area could be related to the grade of severity of OAG disease. We found a significant correlation between HFA MD and CPSD parameters and the N1-P1 mfERG RADs. This suggests that the grade of severity of OAG disease may influence the observed macular dysfunction. By contrast, changes in HFA MD and CPSD did not correlate significantly with the increase of mfERG P1 IT. The lack of significant correlation between the perimetric and the mfERG IT values can be explained by lower intragroup variability in the analysis of IT values: IT SD values were lower than 8% of the mean values, while RADs SD values were greater, with approximately 30%.

In the more external rings (R3–R5, 5–20°), we did not find any statistically significant differences in RADs and ITs between OAG and control eyes. Nevertheless, notwithstanding the presence of normal mfERGs in the more external annular areas tested (5–20°, rings 3–5), the possible presence of isolated areas of retinal dysfunction cannot be entirely excluded. This is supported by data[26,64] showing that when a ring analysis is performed, individual hexagons are not evaluated singly; rather, an average of the bioelectrical responses is obtained from the tested areas. Therefore, some individual abnormal responses could be masked by the adjacent normal responses with consequent normal averaged responses obtained in the entire tested area. This could represent a potential limitation in the ring analysis of mfERG.

In conclusion, our findings lead us to believe that in OAG patients, a dysfunction of the preganglionic elements localized in the foveal area may occur and is detectable by mfERG recordings. Different quantitative changes in this dysfunction may appear at different stages of the glaucoma disease, thus perhaps reflecting a complexity of pathophysiologic mechanisms.[29,65]

Acknowledgments

The authors thank Valter Valli Fiore for technical help in electrophysiological evaluations.

References

1. Parisi V, Falsini B. Electrophysiological evaluation of the macular cone system: focal electroretinography and visual evoked potentials after photostress. *Semin Ophthalmol*. 1998; 13:178–188.
2. Parisi V, Canu D, Iarossi G, Olzi D, Falsini B. Altered recovery of macular function after bleaching in Stargardt's disease-fundus flavimaculatus: pattern VEP evidence. *Invest Ophthalmol Vis Sci*. 2002;43:2741–2748.
3. Parisi V, Pierelli F, Restuccia R, et al. Impaired VEP after photostress response in multiple sclerosis patients previously affected by optic neuritis. *Electroenceph Clin Neurophysiol*. 1998;108:73–79.
4. Seiple WH, Siegel IM, Carr RE, Mayron C. Evaluating macular function using the focal ERG. *Invest Ophthalmol Vis Sci*. 1986; 27:1123–1130.
5. Fish GE, Birch DG. The focal electroretinogram in the clinical assessment of macular disease. *Ophthalmology*. 1989;96:109–114.
6. Miyake Y, Shiroyama N, Horiguchi M, Ota I. Asymmetry of focal ERG in human macular region. *Invest Ophthalmol Vis Sci*. 1989;30:1743–1749.
7. Miyake Y. Focal macular electroretinography. *Nagoya J Med Sci*. 1998;61:79–84.
8. Kondo M, Miyake Y, Kondo N, Ueno S, Takakuwa H, Terasaki H. Peripheral cone dystrophy: a variant of cone dystrophy with predominant dysfunction in the peripheral cone system. *Ophthalmology*. 2004;111:732–739.
9. Binns AM, Margrain TH. Evaluating retinal function in age-related maculopathy with the ERG photostress test. *Invest Ophthalmol Vis Sci*. 2007;48:2806–2813.
10. Parisi V, Bucci MG. Visual evoked potentials after photostress in patients with primary open-angle glaucoma and ocular hypertension. *Invest Ophthalmol Vis Sci*. 1992;33:436–442.
11. Machida S, Tamada K, Oikawa T, Yokoyama D, Kaneko M, Kurosaka D. Sensitivity and specificity of photopic negative response of focal electroretinogram to detect glaucomatous eyes. *Br J Ophthalmol*. 2010;94:202–208.
12. Holopigian K, Seiple W, Mayron C, Koty R, Lorenzo M. Electrophysiological and psychophysical flicker sensitivity in patients with open-angle glaucoma and ocular hypertension. *Invest Ophthalmol Vis Sci*. 1990;31:1863–1868.
13. Porciatti V, Falsini B, Brunori S, Colotto A, Moretti G. Pattern electroretinogram as a function of spatial frequency in ocular hypertension and early glaucoma. *Doc Ophthalmol*. 1987;65: 349–355.
14. Porciatti V, Falsini B. Inner retina contribution to the flicker electroretinogram: a comparison with the pattern electroretinogram. *Clin Vis Sci*. 1993;8:435–447.
15. Falsini B, Colotto A, Porciatti V, Buzzonetti L, Coppè A, De Luca LA. Macular flicker- and pattern-ERGs are differently affected in ocular hypertension and glaucoma. *Clin Vis Sci*. 1991;6:423–429.
16. Weiner A, Ripkin DJ, Patel S, Kaufman SR, Kohn HD, Weidenthal DT. Foveal dysfunction and central visual field loss in glaucoma. *Arch Ophthalmol*. 1998;116:1169–1174.
17. Machida S, Toba Y, Ohtaki A, Gotoh Y, Kaneko M, Kurosaka D. Photopic negative response of focal electroretinograms in glaucomatous eyes. *Invest Ophthalmol Vis Sci*. 2008;49:5636–5644.
18. Sutter EE, Tran D. The field topography of ERG components in man—I. The photopic luminance response. *Vis Res*. 1992;32: 433–446.
19. Hood DC, Odel JG, Chen CS, Winn BJ. The multifocal electroretinogram. *J Neuroophthalmol*. 2003;23:225–235.
20. Varano M, Parisi V, Tedeschi M, et al. Macular function after PDT in myopic maculopathy: psychophysical and electrophysiological evaluation. *Invest Ophthalmol Vis Sci*. 2005;46: 1453–1462.
21. Gerth C, Delahunt PB, Alam S, Morse LS, Werner JS. Cone-mediated multifocal electroretinogram in age-related macular degeneration: progression over a long-term follow-up. *Arch Ophthalmol*. 2006;124:345–352.
22. Parisi V, Ziccardi L, Stifano G, Montrone L, Gallinaro G, Falsini B. Impact of regional retinal responses on cortical visually evoked responses: multifocal ERGs and VEPs in the retinitis pigmentosa model. *Clin Neurophysiol*. 2010;121:380–385.
23. Parisi V, Perillo L, Tedeschi M, et al. Macular function in eyes with early age-related macular degeneration with or without contralateral late age-related macular degeneration. *Retina*. 2007;27:879–890.
24. Parisi V, Tedeschi M, Gallinaro G, et al. Carotenoids and antioxidants in age-related maculopathy Italian study: multifocal electroretinogram modifications after 1 year. *Ophthalmology*. 2008;115:324–333.
25. Bearse MA Jr, Sutter EE. Imaging localized retinal dysfunction with the multifocal electroretinogram. *J Opt Soc Am A Opt Image Sci Vis*. 1996;13:634–640.
26. Hood DC. Assessing retinal function with the multifocal technique. *Prog Retin Eye Res*. 2000;19:607–646.
27. Hood DC, Zhang X. Multifocal ERG and VEP responses and visual fields: comparing disease-related changes. *Doc Ophthalmol*. 2000;100:115–137.

28. Fortune B, Cull G, Wang L, Van Buskirk EM, Cioffi GA. Factors affecting the use of multifocal electroretinography to monitor function in a primate model of glaucoma. *Doc Ophthalmol*. 2002;105:151–178.
29. Fortune B, Johnson CA, Cioffi GA. The topographic relationship between multifocal electroretinographic and behavioral perimetric measures of function in glaucoma. *Optom Vis Sci*. 2001;78:206–214.
30. Chan HH, Brown B. Pilot study of the multifocal electroretinogram in ocular hypertension. *Br J Ophthalmol*. 2000;84: 1147–1153.
31. Chan HH. Detection of glaucomatous damage using multifocal ERG. *Clin Exp Optom*. 2005;88:410–414.
32. Chan HH, Ng YF, Chu PH. Applications of the multifocal electroretinogram in the detection of glaucoma. *Clin Exp Optom*. 2011;94:247–258.
33. Landers J, Sharma A, Goldberg I, Graham S. A comparison of global indices between the Medmont Automated Perimeter and the Humphrey Field Analyzer. *Br J Ophthalmol*. 2007;91: 1285–1287.
34. Shafranov G. Essentials of automated perimetry. In: Walsh T, ed. *Visual Fields Examination and Interpretation*. 3rd ed. New York, NY: Oxford University Press; 2011:94–99.
35. Chylack LT Jr, Wolfe JK, Singer DM, et al. The Lens Opacities Classification System III. The Longitudinal Study of Cataract Study Group. *Arch Ophthalmol*. 1993;111:831–836.
36. Falsini B, Colotto A, Porciatti V, Porrello G. Follow-up study with pattern ERG in ocular hypertension and glaucoma patients under timolol maleate treatment. *Clin Vis Sci*. 1992; 7:341–347.
37. Papst N, Bopp M, Schnaudigel OE. The pattern evoked electroretinogram associated with elevated intraocular pressure. *Graefes Arch Clin Exp Ophthalmol*. 1984;222:34–37.
38. Arden GB, O'Sullivan F. Longitudinal follow up of glaucoma suspects tested with pattern electroretinogram. *Bull Soc Belge Ophtalmol*. 1992;244:147–154.
39. Nesher R, Trick GL, Kass MA, Gordon MO. Steady-state pattern electroretinogram following long term unilateral administration of timolol to ocular hypertensive subjects. *Doc Ophthalmol*. 1990;75:101–109.
40. Colotto A, Salgarello T, Giudiceandrea A, et al. Pattern electroretinogram in treated ocular hypertension: a cross-sectional study after timolol maleate therapy. *Ophthalmic Res*. 1995;27:168–177.
41. Ventura L, Porciatti V. Restoration of retinal ganglion cell function in early glaucoma after intraocular pressure reduction: a pilot study. *Ophthalmology*. 2005;1:20–27.
42. Hood DC, Greenstein VC. Multifocal VEP and ganglion cell damage: applications and limitations for the study of glaucoma. *Prog Retin Eye Res*. 2003;22:201–251.
43. Lachenmayr BJ, Drance SM. Central function and visual field damage in glaucoma. *Int Ophthalmol*. 1992;16:203–209.
44. Kondo M, Miyake Y, Horiguchi M, Suzuki S, Tanikawa A. Clinical evaluation of multifocal electroretinogram. *Invest Ophthalmol Vis Sci*. 1995;36:2146–2150.
45. Hood DC, Frishman LJ, Saszik S, Viswanathan S. Retinal origins of the primate multifocal ERG: implications for the human response. *Invest Ophthalmol Vis Sci*. 2002;43:1673–1685.
46. Bearse Jr MA, Sim D, Sutter EE, et al. Application of the multifocal ERG to glaucoma. *Invest Ophthalmol Vis Sci*. 1996; 37(suppl):S511.
47. Sawada A, Nakazaki S, Nao-i N, Nagatomo A, Arai M. Retinal topography using multifocal electroretinogram in open-angle glaucoma. *Invest Ophthalmol Vis Sci*. 1996;37(suppl):S512.
48. Vaegan, Buckland L. The spatial distribution of ERG losses across the posterior pole of glaucomatous eyes in multifocal recordings. *Aust N Z J Opthalmol*. 1996;24(2 suppl):28–31.
49. Spraul CW, Lang GE, Lang GK, Grossniklaus HE. Morphometric changes of the choriocapillaris and the choroidal vasculature in eyes with advanced glaucomatous changes. *Vision Res*. 2002;42:923–932.
50. Kanis MJ, Lemij HG, Berendschot TT, van de Kraats J, van Norren D. Foveal cone photoreceptor involvement in primary open-angle glaucoma. *Graefes Arch Clin Exp Ophthalmol*. 2010;248:999–1006.
51. Nork TM, Ver Hoeve JN, Poulsen GL, et al. Swelling and loss of photoreceptors in chronic human and experimental glaucomas. *Arch Ophthalmol*. 2000;118:235–245.
52. Pelzel HR, Schlamp CL, Poulsen GL, Ver Hoeve JA, Nork TM, Nickells RW. Decrease of cone opsin mRNA in experimental ocular hypertension. *Mol Vis*. 2006;12:1272–1282.
53. Kendell KR, Quigley HA, Kerrigan LA, Pease ME, Quigley EN. Primary open angle glaucoma is not associated with photoreceptor loss. *Invest Ophthalmol Vis Sci*. 1995;36:200–205.
54. Panda S, Jonas JB. Decreased photoreceptor count in human eyes with secondary angle closure glaucoma. *Invest Ophthalmol Vis Sci*. 1992;33:2532–2536.
55. Karlberg B, Hedin A, Bjornberg K. Electroretinography during short-term intraocular tension rise. *Acta Ophthalmol*. 1968; 46:742–748.
56. Bartl G, Benedikt O, Hiti H, Mandl H. The short-term effect of intraocular pressure elevation on the electrophysiological responses in human eyes. *Albrecht Von Graefes Arch Klin Exp Ophthalmol*. 1974;192:57–64.
57. Viswanathan S, Frishman LJ, Robson JG, Harwerth RS, Smith EL. The photopic negative response of the macaque electroretinogram: reduction by experimental glaucoma. *Invest Ophthalmol Vis Sci*. 1999;40:1124–1136.
58. Hood DC, Greenstein V, Frishman LJ, et al. Identifying inner retinal contributions to the human multifocal ERG. *Vis Res*. 1999;39:2285–2291.
59. Hood DC, Greenstein VC, Holopigian K, et al. An attempt to detect glaucomatous damage to the inner retina with the multifocal ERG. *Invest Ophthalmol Vis Sci*. 2000;41:1570–1579.
60. Hasegawa S, Takagi M, Usui T, Takada R, Abe H. Waveform changes of the first order multifocal electroretinogram in patients with glaucoma. *Invest Ophthalmol Vis Sci*. 2000;41: 1597–1603.
61. Klistorner AI, Graham SL, Martins A. Multifocal pattern electroretinogram does not demonstrate localized field defects in glaucoma. *Doc Ophthalmol*. 2000;100:155–165.
62. Vincent A, Shetty R, Devi SAV, Kurian MK, Balu R, Shetty B. Functional involvement of cone photoreceptors in advanced glaucoma: a multifocal electroretinogram study. *Doc Ophthalmol*. 2010;121:21–27.
63. Brusini P, Filacorda S. Enhanced Glaucoma Staging System (GSS2) for classifying functional damage in glaucoma. *J Glaucoma*. 2006;15:40–46.
64. Li J, Tso MO, Lam TT. Reduced amplitude and delayed latency in foveal response of multifocal electroretinogram in early age related macular degeneration. *Br J Ophthalmol*. 2001;85:287–290.
65. Frishman LJ, Saszik S, Harwerth RS, et al. Effects of experimental glaucoma in macaques on the multifocal ERG. Multifocal ERG in laser-induced glaucoma. *Doc Ophthalmol*. 2000;100:231–251.